

# Pathway-Specific Genetic Attenuation of Glutamate Release Alters Select Features of Competition-Based Visual Circuit Refinement

Selina M. Koch,<sup>1</sup> Cassandra G. Dela Cruz,<sup>2</sup> Thomas S. Hnasko,<sup>3</sup> Robert H. Edwards,<sup>3,4</sup> Andrew D. Huberman,<sup>5</sup> and Erik M. Ullian<sup>2,3,\*</sup>

<sup>1</sup>Neuroscience Graduate Program

<sup>2</sup>Department of Ophthalmology

<sup>3</sup>Department of Physiology

<sup>4</sup>Department of Neurology

University of California, San Francisco, San Francisco, CA 94143, USA

<sup>5</sup>Neurosciences Department, School of Medicine and Neurobiology Section, Division of Biological Sciences, University of California, San Diego, La Jolla, CA 92093, USA

\*Correspondence: ulliane@vision.ucsf.edu

DOI 10.1016/j.neuron.2011.05.045

## SUMMARY

A hallmark of mammalian neural circuit development is the refinement of initially imprecise connections by competitive activity-dependent processes. In the developing visual system retinal ganglion cell (RGC) axons from the two eyes undergo activity-dependent competition for territory in the dorsal lateral geniculate nucleus (dLGN). The direct contributions of synaptic transmission to this process, however, remain unclear. We used a genetic approach to reduce glutamate release selectively from ipsilateral-projecting RGCs and found that their release-deficient axons failed to exclude competing axons from the ipsilateral eye territory in the dLGN. Nevertheless, the release-deficient axons consolidated and maintained their normal amount of dLGN territory, even in the face of fully active competing axons. These results show that during visual circuit refinement glutamatergic transmission plays a direct role in excluding competing axons from inappropriate target regions, but they argue that consolidation and maintenance of axonal territory are largely insensitive to alterations in synaptic activity levels.

## INTRODUCTION

Precise neural circuits are the substrate for cognition, perception, and behavior. In the mammalian nervous system, many neural circuits transition from an imprecise to a refined state to achieve their mature connectivity patterns. The refinement process involves restructuring of axons, dendrites, and synapses such that certain connections are maintained and others are lost. Studies of both CNS and PNS circuits have shown that neural activity can impact circuit refinement through competitive mechanisms in which stronger, more active connections are

maintained and weaker, less active connections are eliminated (Katz and Shatz, 1996; Sanes and Lichtman, 1999).

A long-standing model for probing the mechanisms underlying activity-mediated CNS circuit refinement is the formation of segregated right and left eye axonal projections to the dorsal lateral geniculate nucleus (dLGN). In mammals, axons from the two eyes initially overlap in the dLGN; subsequently, they segregate into nonoverlapping eye-specific territories (Huberman et al., 2008a; Shatz and Sretavan, 1986). Eye-specific segregation involves competition between left and right eye axons that is mediated by spontaneous retinal activity (Penn et al., 1998; Shatz and Sretavan, 1986). If spontaneous activity is perturbed in both eyes or blocked intracranially (Penn et al., 1998; Rossi et al., 2001; Shatz and Stryker, 1988; but see Cook et al., 1999), eye-specific segregation fails to occur. By contrast, if activity is disrupted or increased in one eye, axons from the less active eye lose territory to axons from the more active eye (Koch and Ullian, 2010; Penn et al., 1998; Stellwagen and Shatz, 2002). Thus, the prevailing model is that the relative activity of RGCs in the two eyes dictates which retinogeniculate connections are maintained and which are lost and that this competition is waged through the capacity of RGC axons to drive synaptic plasticity at RGC-dLGN synapses (Butts et al., 2007; Ziburkus et al., 2009). To date, however, few studies have manipulated retino-dLGN transmission *in vivo*; thus the direct roles played by synaptic transmission in eye-specific refinement await determination.

Here we use a mouse genetic strategy to selectively reduce glutamatergic transmission in the developing ipsilateral retinogeniculate pathway *in vivo*. By biasing binocular competition in favor of the axons from the contralateral eye, we were able to directly investigate the role of synaptic competition in activity-dependent neural circuit refinement.

## RESULTS

### Selective Expression of Cre Recombinase in Ipsilateral-Projecting RGCs

To investigate the role of synaptic transmission in visual circuit refinement, we wanted to selectively alter synaptic glutamate

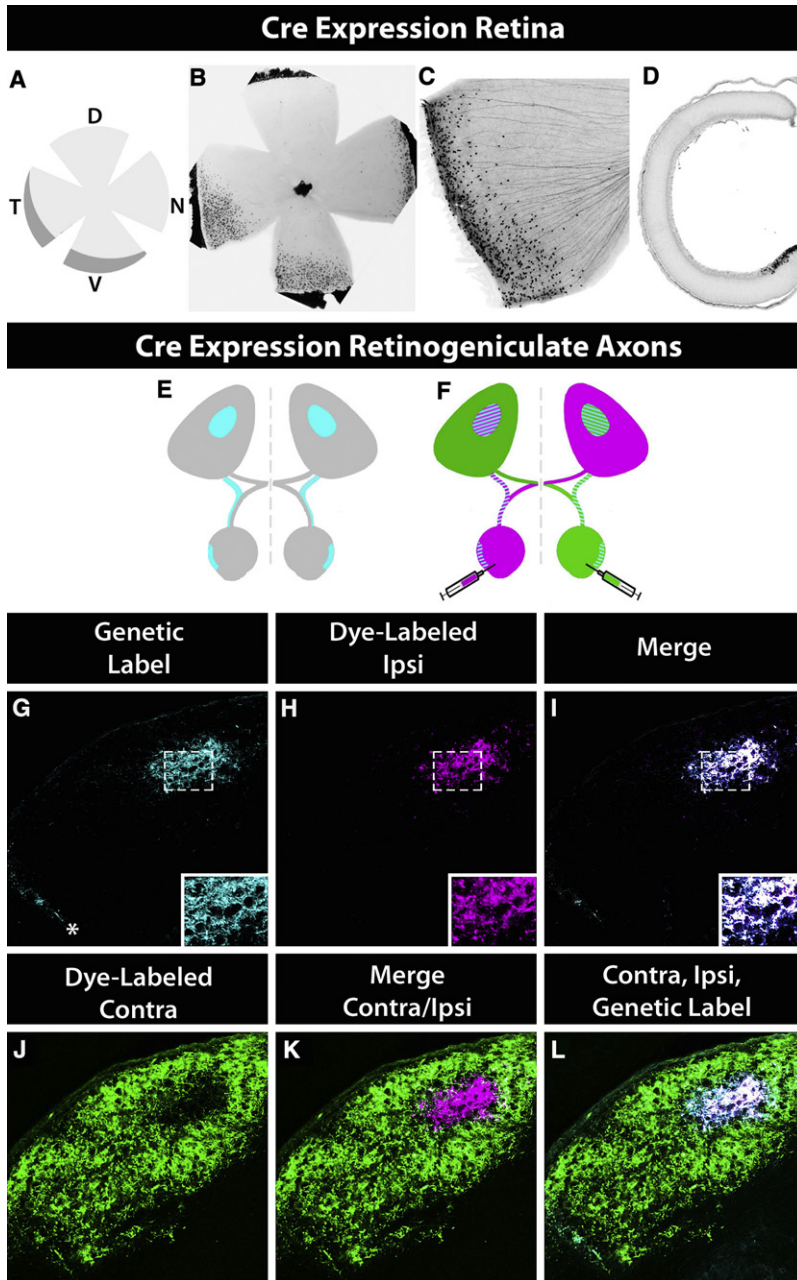


**Figure 1. A Transgenic Mouse that Expresses Cre Selectively in Ipsilateral-Projecting RGCs**

(A) Diagram of a flat mounted retina showing the location of ipsilateral-projecting RGCs in the ventral-temporal periphery (Herrera et al., 2003). (B) X-gal-stained P15 ET33-Cre retina. (C) ET33-Cre::tdTomato axons coursing toward the optic nerve head. (D) Retinal section from a P0 ET33-Cre::tdTomato mouse. (E) Diagram of reporter expression in the retinogeniculate pathway of an ipsilateral-specific Cre animal. (F) Diagram comparing Cre-driven reporter expression to dye-labeled afferents. (G) Cre reporter expression in the dLGN of a P12 ET33 animal (ice blue). Asterisk indicates IGL. (H) Dye-labeled ipsilateral axons (magenta). (I) Merged image showing correspondence between genetically labeled axons and dye-labeled ipsilateral axons (white indicates overlap). (J) Dye-labeled contralateral axons (green). (K) Dye-labeled ipsilateral and contralateral axons. (L) Genetically labeled axons overlaid with dye-labeled ipsilateral and contralateral axons. See also Figure S1.

reporter mice to determine the spatial and temporal pattern of Cre expression.

Ipsilateral-projecting RGCs reside in the ventral-temporal retina (Dräger and Olsen, 1980) (Figure 1A). We therefore examined the location of the Cre-expressing RGCs in retinal flat mounts and transverse sections (Figures 1B–1D). The spatial distribution of the Cre-expressing cells matched the predicted distribution for ipsilateral RGCs (Figures 1B and 1D), plus a thin strip of cells in the dorsal-nasal retina (Figure 1B), a pattern that closely matches SERT expression (García-Frigola and Herrera, 2010). Moreover, most of the Cre-expressing cells were located in the RGC layer (Figure 1D) and extended axons to the optic nerve head, suggesting they were RGCs (Figure 1C).

Next we examined retinogeniculate projections labeled by Cre-driven expression of mGFP or tdTomato and compared them to projections labeled by intraocular injections of the anterograde tracer cholera toxin beta (CTb). If Cre expression is restricted to ipsilateral RGCs one would expect the genetically labeled axons

release from one population of competing RGC axons. Because the serotonin transporter is restricted to the ipsilateral-projecting population of RGCs during development (García-Frigola and Herrera, 2010; Narboux-Nême et al., 2008; Upton et al., 1999), we screened several SERT-Cre lines to determine if any expressed Cre specifically in ipsilateral RGCs (Gong et al., 2007). Because dLGN neurons also express SERT during development (Lebrand et al., 1996), we sought Cre lines with no SERT-Cre expression in the dLGN. One line, ET33 SERT-Cre (see Experimental Procedures), was a promising candidate; consequently, we crossed the ET33 SERT-Cre to various Cre-dependent

to selectively overlap with the CTb-labeled axons from the ipsilateral eye (Figures 1E and 1F). Indeed, that is what we observed (Figures 1I–1L). In addition, a small population of Cre reporter-labeled axons was present in the intergeniculate leaflet (IGL), a thin nucleus that resides between the dLGN and vLGN (Figure 1G). To be certain that the genetically labeled axons arose exclusively from the ipsilateral eye, we removed one eye from an ET33-Cre::tdTomato mouse, allowed 2 weeks for the severed axons to degenerate, and then visualized the intact projections that remained. Axons from the intact eye projected ipsilaterally, whereas the contralateral dLGN was devoid of

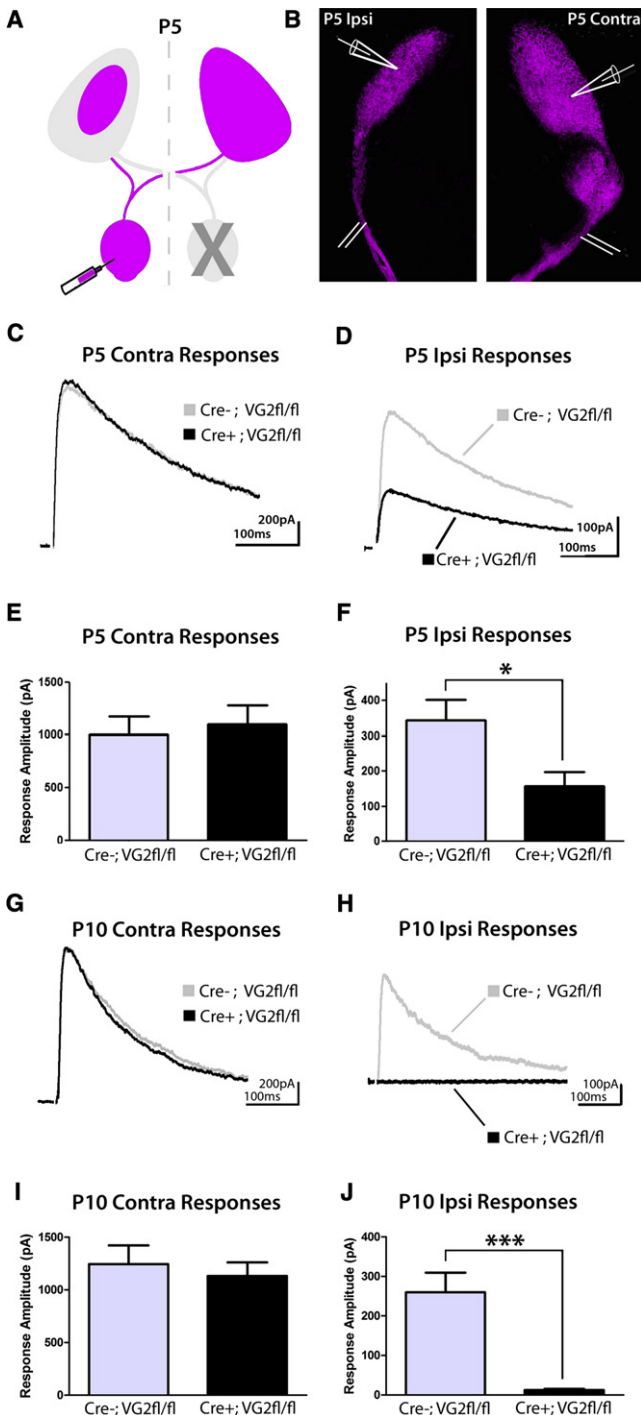


**Figure 2. Conditional Knockout of VGLUT2 in Ipsilateral-Projecting RGCs Selectively Reduces Glutamatergic Synaptic Transmission at Ipsilateral RGC-dLGN Synapses**

(A) Diagram showing removal of one eye and the remaining projections.

(B) Slices containing ipsilateral (left) and contralateral (right) projections and positions of stimulating and recording electrodes.

(C) Example traces from P5 littermates showing NMDAR-mediated responses recorded from dLGN neurons in response to selective stimulation of contralateral axons.

(D) Examples of responses to ipsilateral axon stimulation.

signal (Figure S1B, available online). We also noticed a small Cre-labeled projection to the contralateral IGL (Figure S1B) that probably arose from the small cohort of Cre RGCs in the dorsal-nasal retina (Figure 1B). Importantly, the enucleation experiments also confirmed that little to no Cre expression was apparent in dLGN neurons in ET33-Cre mice (Figure 1I and Figure S1B). Together these data indicate that ET33-Cre is nearly exclusively expressed in ipsilateral-projecting RGCs.

### Pathway-Specific Attenuation of Vesicular Glutamate Release

ET33-Cre mice provide a powerful opportunity to selectively alter gene expression in ipsilateral-projecting RGCs. Because the vesicular glutamate transporter 2 (VGLUT2) is the only vesicular glutamate transporter expressed by RGCs (Fujiyama et al., 2003; Johnson et al., 2003; Sherry et al., 2003; Stella et al., 2008) and is required for synaptic glutamate release (Hnasko et al., 2010; Stuber et al., 2010), we mated ET33-Cre mice with mice that carry floxed alleles of VGLUT2 (Hnasko et al., 2010) in order to generate mice lacking VGLUT2 specifically in ipsilateral-projecting RGCs. In mice, VGLUT2 protein is expressed at low levels at P0 and increases dramatically over the first postnatal week (Sherry et al., 2003; Stella et al., 2008). We found that Cre expression in ET33-Cre mice starts embryonically at least as early as embryonic day 18 (Figure S1C) and when we cultured RGCs from postnatal day 3 (P3) ET33-Cre mice expressing either wild-type or floxed VGLUT2 and immunostained them on P5, we found that VGLUT2 immunofluorescence intensity was nearly absent from the ET33-Cre::VGLUT2<sup>fllox/fllox</sup> RGCs (Figures S2A–S2G).

To determine if retinogeniculate transmission was reduced in ET33-Cre::VGLUT2<sup>fllox/fllox</sup> mice, we measured electrophysiological responses of dLGN neurons in response to optic tract stimulation. We prepared brain slices containing the optic tract and dLGN, which allowed us to stimulate RGC axons and record postsynaptic responses in whole-cell voltage-clamped dLGN neurons (Chen and Regehr, 2000; Koch and Ullian, 2010). The optic tract contains axons from both eyes, so by removing one eye from young mice and allowing the severed RGC axons to degenerate we were able to prepare slices that contained either contralateral or ipsilateral axons, but not both (Figures 2A and 2B). We also injected CTb into the intact eye to visualize its projections in the slice, thus allowing proper targeting of the

(E) Average response amplitudes (in pA) resulting from contralateral axon stimulation at P5 (VGLUT2<sup>fllox/fllox</sup> mice = 1006 ± 138.69 pA, n = 11 and ET33-Cre::VGLUT2<sup>fllox/fllox</sup> mice = 1102 ± 176.1 pA, n = 11; p > 0.05 by Student's t test).

(F) Average amplitudes of ipsilateral responses at P5 (VGLUT2<sup>fllox/fllox</sup> mice = 343.75 ± 59.21 pA, n = 19 and ET33-Cre::VGLUT2<sup>fllox/fllox</sup> mice = 157.49 ± 40.51 pA, n = 22; p = 0.014 by Mann-Whitney U test).

(G) Examples of contralateral responses on P10.

(H) Examples of ipsilateral responses on P10. Note the near complete absence of transmission at this age.

(I) Quantification of P10 contralateral responses (VGLUT2<sup>fllox/fllox</sup> = 1136 ± 126.26 pA, n = 14 and ET33-Cre::VGLUT2<sup>fllox/fllox</sup> = 1136.36 ± 126.19 pA, n = 12; p > 0.05 by Student's t test).

(J) Quantification of P10 ipsilateral responses (VGLUT2<sup>fllox/fllox</sup> = 256.08 ± 49.90 pA, n = 17 and ET33-Cre::VGLUT2<sup>fllox/fllox</sup> = 7.54 ± 3.60 pA, n = 22; p < 0.0001 by Mann-Whitney U test).

Error bars in (E), (F), (I), and (J) indicate SEM. See also Figure S2.

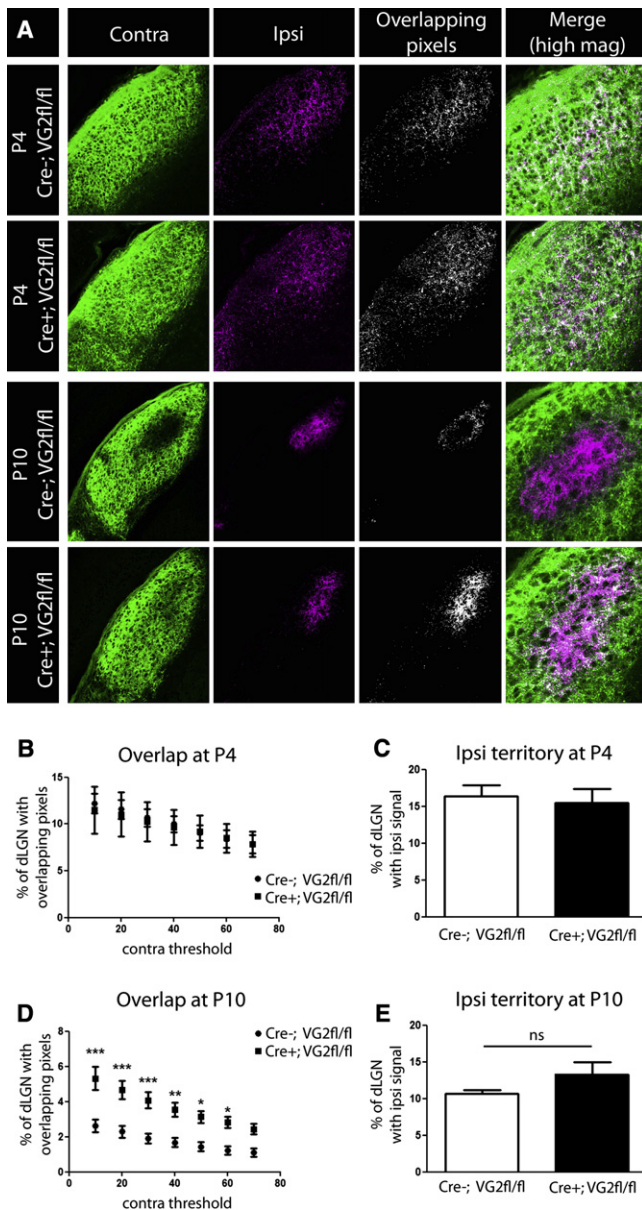


**Figure 3. Diminished Ipsilateral Synaptic Transmission Perturbs Eye-Specific Segregation but Not Consolidation of Ipsilateral Eye Territory in the dLGN**

(A) Images showing dye-labeled retinogeniculate axons in control and ET33-Cre::VGLUT2<sup>flox/flox</sup> animals on P4 (upper two rows) and P10 (lower two rows). The first column shows contralateral axons (green) and the second column shows ipsilateral axons (magenta). The third column shows the pixels with overlapping contralateral and ipsilateral signal (white). The fourth column shows a higher magnification image of the region of overlap (white indicates overlap).

(B) Percentage of dLGN pixels that displayed overlapping contralateral and ipsilateral signal on P4 (n = 6 mice per genotype). Two-way ANOVA revealed no significant differences over a range of noise thresholds.

(C) Amount of ipsilateral eye territory as a fraction of the total dLGN area on P4. (D) Overlap of contralateral and ipsilateral axons on P10 (\*\*p < 0.001, \*\*\*p < 0.01, \*p < 0.05 by two-way ANOVA, n = 8 mice per genotype).

(E) Amount of ipsilateral signal on P10 (ipsilateral eye axons occupied 10.68 ± 0.44% of the dLGN in VGLUT2<sup>flox/flox</sup> animals and 13.03 ± 1.63% in

recording and stimulating electrodes (Figure 2B). Recordings were performed on P5 and P10.

Stimulation of contralateral RGC axons in P5 slices produced postsynaptic NMDAR-mediated responses in every dLGN neuron tested, regardless of genotype. Indeed, the size of the contralateral NMDAR-mediated responses was indistinguishable between Cre-expressing and Cre-negative slices (Figures 2C and 2E; VGLUT2<sup>flox/flox</sup> = 1006 ± 138.69 pA, n = 11 and ET33-Cre::VGLUT2<sup>flox/flox</sup> = 1102 ± 176.1 pA, n = 11; p > 0.05 by Student's t test). By contrast, when ipsilateral RGC axons were stimulated, dLGN neurons in ET33-Cre::VGLUT2<sup>flox/flox</sup> slices often failed to respond (11 responses out of 24 cells) and response sizes were reduced by ~55% (Figures 2D and 2F; VGLUT2<sup>flox/flox</sup> mice = 343.75 ± 59.21 pA, n = 19 and ET33-Cre::VGLUT2<sup>flox/flox</sup> mice = 157.49 ± 40.51 pA, n = 22; p = 0.014 by Mann-Whitney U test). AMPAR-mediated responses showed similar results (Figures S2H–S2M).

Next we assessed retinogeniculate transmission in slices from P10 mice, an age when ongoing spontaneous activity continues to refine and maintain eye-specific retinogeniculate projections (Chapman, 2000; Demas et al., 2006). Similar to what was observed on P5, the contralateral responses of P10 dLGN neurons were identical between ET33-Cre::VGLUT2<sup>flox/flox</sup> animals and controls (Figures 2G and 2I; VGLUT2<sup>flox/flox</sup> = 1136 ± 126.26 pA, n = 14 and ET33-Cre::VGLUT2<sup>flox/flox</sup> = 1136.36 ± 126.19 pA, n = 12; p > 0.05 by Student's t test), whereas ipsilateral responses were significantly reduced (Figures 2H and 2J; VGLUT2<sup>flox/flox</sup> = 256.08 ± 49.90 pA, n = 17 and ET33-Cre::VGLUT2<sup>flox/flox</sup> = 7.54 ± 3.60 pA, n = 22; p < 0.0001 by Mann-Whitney U test). In P10 ET33-Cre::VGLUT2<sup>flox/flox</sup> slices, only 18% of dLGN neurons responded to ipsilateral axon stimulation (4 of 22 compared to 17 of 19 in controls) and their average response sizes were reduced by 97%. AMPAR-mediated ipsilateral responses were also further reduced between P5 and P10 (Figures S2H–S2M). Collectively, our electrophysiological findings demonstrate that glutamatergic synaptic transmission is selectively and progressively reduced in the ipsilateral retinogeniculate pathway of early postnatal ET33-Cre::VGLUT2<sup>flox/flox</sup> mice.

### Attenuation of Glutamatergic Transmission Impacts Select Aspects of Retinogeniculate Refinement

What role does synaptic competition play in eye-specific retinogeniculate refinement? To address this question, we analyzed ipsilateral and contralateral projections at different developmental stages in ET33-Cre::VGLUT2<sup>flox/flox</sup> animals by labeling axons from each eye with CTb-488 or CTb-594. In wild-type mice, ipsilateral and contralateral axon territories overlap in the dLGN at P4 (Godement et al., 1984; Jaubert-Miazza et al., 2005) and we found that on P4 both Cre-negative and Cre-expressing VGLUT2<sup>flox/flox</sup> littermates exhibited overlapping axonal projection patterns typical for this age (Figures 3A–3C).

In wild-type mice, eye-specific territories are clearly visible by P10 (Godement et al., 1984; Jaubert-Miazza et al., 2005;

ET33-Cre::VGLUT2<sup>flox/flox</sup> animals, n = 8 mice per genotype; p > 0.05 by Student's t test).

Error bars in (B)–(D) indicate SEM. See also Figure S3.

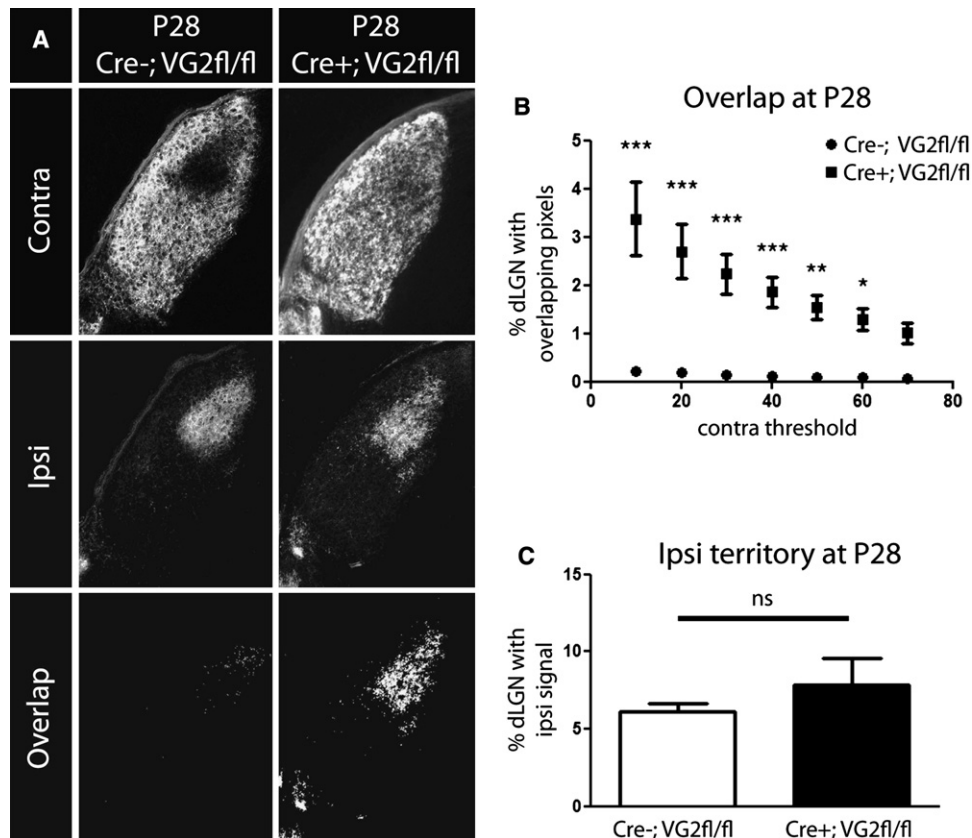


**Figure 4. Ipsilateral Retinogeniculate Axons Maintain Target Territory despite Prolonged Reduction in Glutamatergic Synaptic Transmission**

(A) Examples showing retinogeniculate projections at P28 in a VGLUT2<sup>flox/flox</sup> animal (left column) and an ET33-Cre::VGLUT2<sup>flox/flox</sup> littermate (right column). The Cre+ animal continues to exhibit contralateral axons (top row) throughout the entire dLGN, a robust ipsilateral projection (middle row), and a high degree of overlap between contralateral and ipsilateral axons (bottom).

(B) Overlap on P28 (\*\**p* < 0.001, \*\**p* < 0.01, \**p* < 0.05 by two-way ANOVA, *n* = 7 mice per genotype).

(C) Amount of ipsilateral signal on P28 (ipsilateral eye axons occupied 6.10 ± 0.56% of the dLGN in VGLUT2<sup>flox/flox</sup> animals and 7.84 ± 1.73% in ET33-Cre::VGLUT2<sup>flox/flox</sup> animals, *n* = 7 mice per genotype; *p* > 0.05 by Mann-Whitney U test). Error bars in (B) and (C) indicate SEM.

Muir-Robinson et al., 2002) (Figure 3A). Based on previous studies (Penn et al., 1998; Stellwagen and Shatz, 2002), we predicted that the synaptically weakened ipsilateral axons would fail to outcompete and eject contralateral axons from their territory and that the ipsilateral eye territory would be reduced. Indeed, we found that in the ET33-Cre::VGLUT2<sup>flox/flox</sup> mice, contralateral eye axons failed to retract from the ipsilateral region of the dLGN (Figure 3A), resulting in a greater than normal degree of overlap between ipsilateral and contralateral axons (Figure 3D; *n* = 8 mice for each genotype). The increased overlap was significant over a wide range of signal-to-noise thresholds (Figure 3D) (see Experimental Procedures). The abnormal degree of overlap did not occur in animals expressing ET33-Cre alone or ET33-Cre and one floxed VGLUT2 allele (Figure S3D). These data provide evidence that effective glutamatergic transmission is crucial for mediating axon-axon competition during CNS refinement.

Surprisingly, however, reducing ipsilateral synaptic transmission did not alter the overall pattern of the ipsilateral terminal field (Figures 3A and 3E and Figure S3). The ipsilateral eye axons were completely intermingled with contralateral eye axons and yet, with respect to overall size, shape, and position,

ET33-Cre::VGLUT2<sup>flox/flox</sup> mice displayed ipsilateral projections that were indistinguishable from that of control mice (Figure 3E and Figure S3). Ipsilateral eye axons occupied 10.68 ± 0.44% of the dLGN in controls and 13.03 ± 1.63% in ET33-Cre::VGLUT2<sup>flox/flox</sup> animals (*n* = 8 mice for each genotype, *p* > 0.05 by Student's *t* test). Thus, despite having markedly reduced glutamate release throughout the major phase of eye-specific segregation (Figure 2), ipsilateral eye axons were still able to consolidate their normal amount of dLGN territory (Figures 3A and 3D and Figure S3).

Spontaneous retinal activity continues beyond P10 and is necessary to maintain eye-specific dLGN territories (Bansal et al., 2000; Chapman, 2000; Demas et al., 2006). We therefore asked whether normal levels of glutamatergic transmission are necessary to maintain the ipsilateral eye territory in ET33-Cre::VGLUT2<sup>flox/flox</sup> mice. On P28, contralateral RGC axons were distributed throughout the entire dLGN in ET33-Cre::VGLUT2<sup>flox/flox</sup> mice (Figures 4A and 4B; *n* = 7 mice per genotype), similar to the pattern observed in these mice on P10, further indicating that normal levels of glutamate release are crucial for appropriate CNS circuit refinement. However, despite

having been at a competitive disadvantage since at least P5, the size of the ipsilateral eye territory was not diminished in P28 ET33-Cre::VGLUT2<sup>flox/flox</sup> animals (Figures 4A and 4C). Ipsilateral eye axons consisted of  $6.10 \pm 0.56\%$  of the dLGN in controls and  $7.84 \pm 1.73\%$  in ET33-Cre::VGLUT2<sup>flox/flox</sup> animals ( $n = 7$  mice for each genotype,  $p > 0.05$  by Mann-Whitney U test). The fact that the patterning of the ipsilateral eye territory in the dLGN was refractory to reductions in glutamate release both during and after the period of eye-specific segregation is surprising as it stands in bold contrast to current models of activity-dependent retinogeniculate refinement (reviewed in Huberman et al., 2008a) (Figure S4).

## DISCUSSION

We found that reducing glutamatergic synaptic currents profoundly altered certain aspects of RGC axon remodeling, whereas other aspects were unaffected. While reduced ipsilateral transmission led to an abnormal persistence of competing contralateral eye axons in the ipsilateral eye territory (Figures 3A and 3D), it did not prevent ipsilateral eye axons from (1) targeting to the appropriate region of the dLGN (Figure 3A), (2) refining into a normally sized termination zone (Figures 3A and 3E), and (3) maintaining that territory into the late postnatal period (Figures 4A and 4C). The ability of the release-deficient axons to consolidate and maintain their normal amount of target territory in the face of more active competing axons is surprising in light of previous studies (Chapman, 2000; Demas et al., 2006; Penn et al., 1998; Stellwagen and Shatz, 2002). The finding is, however, reminiscent of results from studies of cortical ocular dominance column development, which demonstrated that early on there is a strong functional bias in favor of contralateral eye connections and yet, that bias does not prevent axons representing the ipsilateral eye from consolidating cortical territory (Crair et al., 1998, 2001).

An important caveat of our experimental manipulation is that it did not eliminate glutamate release completely. The present study, therefore, cannot determine if glutamate release is necessary for axon territory consolidation and maintenance. In addition, it is not presently possible to measure the effects of VGLUT2 reduction on RGC-dLGN transmission patterns *in vivo*; therefore, a full assessment of the synaptic defects present in ET33-Cre::VGLUT2<sup>flox/flox</sup> mice during retinal waves remains to be determined. As it stands, the residual glutamate release observed in ET33-Cre::VGLUT2<sup>flox/flox</sup> mice at P5 may be sufficient to stabilize and refine their ipsilateral RGC axons, whereas the mechanism that eliminates competing axons may be more sensitive to alterations in glutamate release.

Why would ipsilateral axons refine normally with diminished VGLUT2 (Figure 3), whereas monocular activity perturbations lead to a reduced ipsilateral eye territory (Koch and Ullian, 2010; Penn et al., 1998)? The differences in those outcomes may reflect differences between the experimental manipulations in the studies. While VGLUT2 reduction weakened retinogeniculate transmission during eye-specific segregation (Figure 2), intraocular epibatidine treatment altered RGC spiking patterns (Penn et al., 1998; Sun et al., 2008), which in theory should cause abnormal transmission patterns at RGC-dLGN synapses.

Abnormal patterns of synaptic activity may lead to a punishment signal that causes axons to be lost, whereas axons with dramatically weakened (or abolished) synaptic currents may fail to elicit or respond to such a signal. Another potential explanation is that in addition to evoking glutamate release from RGC axons, retinal waves cause calcium influxes in RGCs. Therefore, manipulations that alter spontaneous retinal activity patterns may exert broader effects on RGC axons than does VGLUT2 reduction. A third possibility is that RGC axons may release factors other than glutamate to control the consolidation of their target territory and those factors may be differentially impacted by epibatidine versus VGLUT2 reduction. For instance, RGCs express the vesicular monoamine transporter 2 (VMAT2) during development and the very promoter used to drive Cre expression in ipsilateral RGCs—SERT—is specifically expressed by ipsilateral RGCs during development (Upton et al., 1999; García-Frigola and Herrera, 2010). Indeed, eye-specific layers fail to form in animals lacking monoamine oxidase or SERT (Upton et al., 1999). In the future it will be interesting to address whether removal of SERT from VGLUT2-depleted RGCs would disrupt the ability of ipsilateral RGCs to consolidate and maintain dLGN territory.

In summary, our data demonstrate a key role for glutamatergic synaptic transmission during CNS circuit refinement in mediating the exclusion of axons from inappropriate target regions. However, contrary to what current models of activity-dependent development would predict, our data also demonstrate that RGC populations with markedly reduced synaptic activity can still consolidate and maintain normal amounts of target territory, even in the presence of more active competitors. These findings advance our understanding of the mechanisms that establish developing CNS circuits by helping to clarify the direct contributions of glutamatergic synaptic transmission to axon refinement.

## EXPERIMENTAL PROCEDURES

### Mouse Lines

The ET33 Sert-Cre line was generated by GENSAT (Gong et al., 2007) and obtained from Mutant Mouse Regional Resource Centers (<http://www.mmrrc.org/strains/17260/017260.html>). The lox-STOP-lox-mGFP-IRES-NLS-LacZ-pA reporter (Hippenmeyer et al., 2005) was a gift from J.L. Rubenstein (University of California, San Francisco) and lox-STOP-lox-lacZ (Soriano, 1999) and lox-STOP-lox-tdTomato (Ai9; Madisen et al., 2010) were obtained from The Jackson Laboratory. Homozygous floxed VGLUT2 mice were previously described (Hnasko et al., 2010). All mouse lines were congenic on the C57BL/6 background except for the mGFP mice, which were on a mixed 129SV/J and C57BL/6 background.

### Retinal and Brain Histology

Eyes were removed and fixed in 4% PFA for 8 hr at 4°C. Retinal whole mounts were prepared by extracting the retina from the eye. Retinal sections were prepared by hemisecting fixed eyes, cryoprotecting the sections in 30% sucrose, freezing them, and cryosectioning them at 12 μm. LGN histology: brains were fixed overnight in 4% PFA at 4°C, cryoprotected in 30% sucrose, and sectioned in the coronal plane at 40 μm. X-gal staining: retinas were washed in buffer (0.0015 M MgCl<sub>2</sub>, 0.01% deoxycholate, and 0.02% NP40 in phosphate buffer) three times for 15 min, placed in stain (2.45 mM X-gal in dimethylformamide, 5.0 mM potassium ferrocyanide, and 5.0 mM potassium ferricyanide in wash buffer) for 2 hr at 37°C, and washed again three times for 15 min. Visualization of mGFP reporter was performed as described (Huberman et al., 2008b). Imaging the tdTomato reporter did not require immunostaining.

**Retinal Cell Culture and Immunocytochemistry**

Retinas were harvested from P3 mice, digested with papain (16.5 U/ml; Worthington), dissociated, and plated on glass coverslips (coated with 10 mg/ml poly-D-lysine and 2 mg/ml laminin) at 25,000 cells/well in a 24-well plate. Cells were incubated in defined media (Meyer-Franke et al., 1995).

At DIV 2, cultured retinal cells were fixed in 4% paraformaldehyde, rinsed in PBS, and blocked for 30 min in a 1:1 mix of goat serum and antibody buffer (150 mM NaCl, 50 mM Tris base, 1% L-lysine, and 0.4% azide). Cells were incubated in guinea pig anti-VGLUT2 polyclonal antibody (1:1500, Millipore) overnight at 4°C and then rinsed in PBS three times for 10 min. Alexa Fluor 488 goat anti-guinea pig secondary (1:500, Invitrogen) was applied at room temperature for 1.5 hr followed by three rinses in PBS and mounting in Vectashield.

Cells were imaged at 20 × on a Zeiss Axio Imager.M1 microscope. All images were imported into Adobe Photoshop and thresholded. ET33-Cre-expressing cells were identified by their tdTomato expression. The somas of Cre-expressing cells were outlined and the average fluorescence intensity of the VGLUT2 signal within the traced area was measured by using the histogram function. VGLUT2 fluorescence intensity was normalized to soma size for each cell. Data were compared by a Student's t test.

**Electrophysiology**

One retina was removed on either P0 or P5 and recordings were performed on P5 or P10, respectively. Brain sections (325 μm) containing the optic tract and dLGN were acutely prepared as previously described (Chen and Regehr, 2000; Koch and Ullian, 2010; Bickford et al., 2010). Sectioning was performed in oxygenated cutting solution consisting of 78.3 mM NaCl, 23.0 mM NaHCO<sub>3</sub>, 23.0 mM dextrose, 33.8 mM choline chloride, 2.3 mM KCl, 1.1 mM NaH<sub>2</sub>PO<sub>4</sub>, 6.4 mM MgCl<sub>2</sub>, and 0.45 mM CaCl<sub>2</sub>. Brains were incubated for 25 min at 34°C in cutting solution and then transferred to oxygenated ACSF consisting of 125.0 mM NaCl, 25.0 mM NaHCO<sub>3</sub>, 25.0 mM dextrose, 2.5 mM KCl, 1.25 mM NaH<sub>2</sub>PO<sub>4</sub>, 2.0 mM CaCl<sub>2</sub>, and 1.0 MgCl<sub>2</sub> × 6H<sub>2</sub>O. Recordings were made at room temperature.

Whole-cell voltage-clamp recordings of dLGN neurons were obtained by using 2.5–3.5 MΩ patch electrodes containing internal solution (35 mM CsF, 100 mM CsCl, 10 mM EGTA, and 10 mM HEPES). Inhibitory inputs were blocked with 20 μM bicuculline methobromide (Tocris). Recordings were sampled at 10–20 kHz and filtered at 1 kHz. Access resistance was monitored and adjusted to 4–9 MΩ after 70% compensation. A concentric bipolar stimulating electrode was placed just touching the surface of the optic tract next to the ventral LGN and a 1 ms stimulus was delivered every 30 s. A 40 μA stimulus was used because this intensity evoked action potentials from many RGC axons, typically resulting in maximal postsynaptic responses in control cells. NMDAR-mediated current amplitudes were measured at +40 mV and at a time when the AMPAR-mediated currents no longer contributed to the response, ~25 ms after the onset of the EPSC. Synaptic currents were analyzed by using Igor Pro, Microsoft Excel, and GraphPad Prism programs. All experiments and analyses were done blind to genotype. Statistical comparisons were made by using a Student's unpaired t test unless otherwise stated.

**Dye-Labeling Retinogeniculate Axons**

Mice were anesthetized with isoflurane and their eyelids were gently separated with tweezers. Eyes were numbed with proparacaine and injected with 1.0–2.0 μL of CTb-488 or CTb-594 (0.5% in sterile saline), 1.0 μL for P3 mice, 1.5 μL for P9 mice, and 2.0 μL for P27 mice.

**Analysis of Retinogeniculate Projections**

Confocal images of dLGN sections were acquired on an Axiovert 200 microscope and Pascal acquisition software. Two sections from the center of the dLGN on both sides of the brain were averaged per animal. Images were thresholded in Adobe Photoshop and imported into ImageJ and the boundary of the dLGN was delineated in order to exclude label from the optic tract and IGL. The area occupied by the ipsilateral axons was measured by comparing all ipsilateral signal-containing pixels within the dLGN to the total number of dLGN pixels. For binocular overlap the binary ipsilateral and contralateral images were multiplied in Photoshop (yielding images containing only the

overlapped signal) and imported into ImageJ for comparison of overlapping signal within the dLGN. Analysis of axonal overlap was performed over a range of signal-to-noise thresholds (Bjartmar et al., 2006; Rebsam et al., 2009; Torborg et al., 2005).

**SUPPLEMENTAL INFORMATION**

Supplemental Information includes four figures and can be found with this article online at doi:10.1016/j.neuron.2011.05.045.

**ACKNOWLEDGMENTS**

We thank Phong Nguyen for expert technical assistance. This work was supported by NIMH-MH50712 (R.H.E.), The E. Matilda Zigler Foundation for the Blind (A.D.H.), T32-EY07120 (S.M.K.), Research to Prevent Blindness and March of Dimes (E.M.U.), NEI-EY002162, and a Research to Prevent Blindness Unrestricted Grant.

Accepted: May 26, 2011

Published: July 27, 2011

**REFERENCES**

- Bansal, A., Singer, J.H., Hwang, B.J., Xu, W., Beaudet, A., and Feller, M.B. (2000). Mice lacking specific nicotinic acetylcholine receptor subunits exhibit dramatically altered spontaneous activity patterns and reveal a limited role for retinal waves in forming ON and OFF circuits in the inner retina. *J. Neurosci.* 20, 7672–7681.
- Bickford, M.E., Slusarczyk, A., Dilger, E.K., Krahe, T.E., Kucuk, C., and Guido, W. (2010). Synaptic development of the mouse dorsal lateral geniculate nucleus. *J. Comp. Neurol.* 518, 622–635.
- Bjartmar, L., Huberman, A.D., Ullian, E.M., Rentería, R.C., Liu, X., Xu, W., Prezioso, J., Susman, M.W., Stellwagen, D., Stokes, C.C., et al. (2006). Neuronal pentraxins mediate synaptic refinement in the developing visual system. *J. Neurosci.* 26, 6269–6281.
- Butts, D.A., Kanold, P.O., and Shatz, C.J. (2007). A burst-based “Hebbian” learning rule at retinogeniculate synapses links retinal waves to activity-dependent refinement. *PLoS Biol.* 5, e61.
- Chapman, B. (2000). Necessity for afferent activity to maintain eye-specific segregation in ferret lateral geniculate nucleus. *Science* 287, 2479–2482.
- Chen, C., and Regehr, W.G. (2000). Developmental remodeling of the retinogeniculate synapse. *Neuron* 28, 955–966.
- Cook, P.M., Prusky, G., and Ramoa, A.S. (1999). The role of spontaneous retinal activity before eye opening in the maturation of form and function in the retinogeniculate pathway of the ferret. *Vis. Neurosci.* 16, 491–501.
- Crair, M.C., Gillespie, D.C., and Stryker, M.P. (1998). The role of visual experience in the development of columns in cat visual cortex. *Science* 279, 566–570.
- Crair, M.C., Horton, J.C., Antonini, A., and Stryker, M.P. (2001). Emergence of ocular dominance columns in cat visual cortex by 2 weeks of age. *J. Comp. Neurol.* 430, 235–249.
- Demas, J., Sagdullaev, B.T., Green, E., Jaubert-Miazza, L., McCall, M.A., Gregg, R.G., Wong, R.O., and Guido, W. (2006). Failure to maintain eye-specific segregation in nob, a mutant with abnormally patterned retinal activity. *Neuron* 50, 247–259.
- Dräger, U.C., and Olsen, J.F. (1980). Origins of crossed and uncrossed retinal projections in pigmented and albino mice. *J. Comp. Neurol.* 191, 383–412.
- Fujiyama, F., Hioki, H., Tomioka, R., Taki, K., Tamamaki, N., Nomura, S., Okamoto, K., and Kaneko, T. (2003). Changes of immunocytochemical localization of vesicular glutamate transporters in the rat visual system after the retinofugal denervation. *J. Comp. Neurol.* 465, 234–249.
- García-Frigola, C., and Herrera, E. (2010). Zic2 regulates the expression of Sert to modulate eye-specific refinement at the visual targets. *EMBO J.* 29, 3170–3183.

- Godement, P., Salaün, J., and Imbert, M. (1984). Prenatal and postnatal development of retinogeniculate and retinocollicular projections in the mouse. *J. Comp. Neurol.* 230, 552–575.
- Gong, S., Doughty, M., Harbaugh, C.R., Cummins, A., Hatten, M.E., Heintz, N., and Gerfen, C.R. (2007). Targeting Cre recombinase to specific neuron populations with bacterial artificial chromosome constructs. *J. Neurosci.* 27, 9817–9823.
- Herrera, E., Brown, L., Aruga, J., Rachel, R.A., Dolen, G., Mikoshiba, K., Brown, S., and Mason, C.A. (2003). *Zic2* patterns binocular vision by specifying the uncrossed retinal projection. *Cell* 114, 545–557.
- Hippenmeyer, S., Vrieseling, E., Sigrist, M., Portmann, T., Laengle, C., Ladle, D.R., and Arber, S. (2005). A developmental switch in the response of DRG neurons to ETS transcription factor signaling. *PLoS Biol.* 3, e159.
- Hnasko, T.S., Chuhma, N., Zhang, H., Goh, G.Y., Sulzer, D., Palmiter, R.D., Rayport, S., and Edwards, R.H. (2010). Vesicular glutamate transport promotes dopamine storage and glutamate corelease in vivo. *Neuron* 65, 643–656.
- Huberman, A.D., Feller, M.B., and Chapman, B. (2008a). Mechanisms underlying development of visual maps and receptive fields. *Annu. Rev. Neurosci.* 31, 479–509.
- Huberman, A.D., Manu, M., Koch, S.M., Susman, M.W., Lutz, A.B., Ullian, E.M., Baccus, S.A., and Barres, B.A. (2008b). Architecture and activity-mediated refinement of axonal projections from a mosaic of genetically identified retinal ganglion cells. *Neuron* 59, 425–438.
- Jaubert-Miazza, L., Green, E., Lo, F.S., Bui, K., Mills, J., and Guido, W. (2005). Structural and functional composition of the developing retinogeniculate pathway in the mouse. *Vis. Neurosci.* 22, 661–676.
- Johnson, J., Tian, N., Caywood, M.S., Reimer, R.J., Edwards, R.H., and Copenhagen, D.R. (2003). Vesicular neurotransmitter transporter expression in developing postnatal rodent retina: GABA and glycine precede glutamate. *J. Neurosci.* 23, 518–529.
- Katz, L.C., and Shatz, C.J. (1996). Synaptic activity and the construction of cortical circuits. *Science* 274, 1133–1138.
- Koch, S.M., and Ullian, E.M. (2010). Neuronal pentraxins mediate silent synapse conversion in the developing visual system. *J. Neurosci.* 30, 5404–5414.
- Lebrand, C., Cases, O., Adelbrecht, C., Doye, A., Alvarez, C., El Mestikawy, S., Seif, I., and Gaspar, P. (1996). Transient uptake and storage of serotonin in developing thalamic neurons. *Neuron* 17, 823–835.
- Madisen, L., Zwingman, T.A., Sunkin, S.M., Oh, S.W., Zariwala, H.A., Gu, H., Ng, L.L., Palmiter, R.D., Hawrylycz, M.J., Jones, A.R., et al. (2010). A robust and high-throughput Cre reporting and characterization system for the whole mouse brain. *Nat. Neurosci.* 13, 133–140.
- Meyer-Franke, A., Kaplan, M.R., Pfrieger, F.W., and Barres, B.A. (1995). Characterization of the signaling interactions that promote the survival and growth of developing retinal ganglion cells in culture. *Neuron* 15, 805–819.
- Muir-Robinson, G., Hwang, B.J., and Feller, M.B. (2002). Retinogeniculate axons undergo eye-specific segregation in the absence of eye-specific layers. *J. Neurosci.* 22, 5259–5264.
- Narboux-Nême, N., Pavone, L.M., Avallone, L., Zhuang, X., and Gaspar, P. (2008). Serotonin transporter transgenic (SERT<sup>Cre</sup>) mouse line reveals developmental targets of serotonin specific reuptake inhibitors (SSRIs). *Neuropharmacology* 55, 994–1005.
- Penn, A.A., Riquelme, P.A., Feller, M.B., and Shatz, C.J. (1998). Competition in retinogeniculate patterning driven by spontaneous activity. *Science* 279, 2108–2112.
- Rebsam, A., Petros, T.J., and Mason, C.A. (2009). Switching retinogeniculate axon laterality leads to normal targeting but abnormal eye-specific segregation that is activity dependent. *J. Neurosci.* 29, 14855–14863.
- Rossi, F.M., Pizzorusso, T., Porciatti, V., Marubio, L.M., Maffei, L., and Changeux, J.P. (2001). Requirement of the nicotinic acetylcholine receptor beta 2 subunit for the anatomical and functional development of the visual system. *Proc. Natl. Acad. Sci. USA* 98, 6453–6458.
- Sanes, J.R., and Lichtman, J.W. (1999). Development of the vertebrate neuromuscular junction. *Annu. Rev. Neurosci.* 22, 389–442.
- Shatz, C.J., and Sretavan, D.W. (1986). Interactions between retinal ganglion cells during the development of the mammalian visual system. *Annu. Rev. Neurosci.* 9, 171–207.
- Shatz, C.J., and Stryker, M.P. (1988). Prenatal tetrodotoxin infusion blocks segregation of retinogeniculate afferents. *Science* 242, 87–89.
- Sherry, D.M., Wang, M.M., Bates, J., and Frishman, L.J. (2003). Expression of vesicular glutamate transporter 1 in the mouse retina reveals temporal ordering in development of rod vs. cone and ON vs. OFF circuits. *J. Comp. Neurol.* 465, 480–498.
- Soriano, P. (1999). Generalized lacZ expression with the ROSA26 Cre reporter strain. *Nat. Genet.* 21, 70–71.
- Stella, S.L., Jr., Li, S., Sabatini, A., Vila, A., and Brecha, N.C. (2008). Comparison of the ontogeny of the vesicular glutamate transporter 3 (VGLUT3) with VGLUT1 and VGLUT2 in the rat retina. *Brain Res.* 1215, 20–29.
- Stellwagen, D., and Shatz, C.J. (2002). An instructive role for retinal waves in the development of retinogeniculate connectivity. *Neuron* 33, 357–367.
- Stuber, G.D., Hnasko, T.S., Britt, J.P., Edwards, R.H., and Bonci, A. (2010). Dopaminergic terminals in the nucleus accumbens but not the dorsal striatum corelease glutamate. *J. Neurosci.* 30, 8229–8233.
- Sun, C., Speer, C.M., Wang, G.Y., Chapman, B., and Chalupa, L.M. (2008). Epibatidine application in vitro blocks retinal waves without silencing all retinal ganglion cell action potentials in developing retina of the mouse and ferret. *J. Neurophysiol.* 100, 3253–3263.
- Torborg, C.L., Hansen, K.A., and Feller, M.B. (2005). High frequency, synchronized bursting drives eye-specific segregation of retinogeniculate projections. *Nat. Neurosci.* 8, 72–78.
- Upton, A.L., Salichon, N., Lebrand, C., Ravary, A., Blakely, R., Seif, I., and Gaspar, P. (1999). Excess of serotonin (5-HT) alters the segregation of ipsilateral and contralateral retinal projections in monoamine oxidase A knock-out mice: possible role of 5-HT uptake in retinal ganglion cells during development. *J. Neurosci.* 19, 7007–7024.
- Ziburkus, J., Dilger, E.K., Lo, F.S., and Guido, W. (2009). LTD and LTP at the developing retinogeniculate synapse. *J. Neurophysiol.* 102, 3082–3090.